

Effect of residual catalyst on the vibrational modes of single-walled carbon nanotubes

L. E. McNeil,^{a)} H. Park, and J. P. Lu

Department of Physics and Astronomy, University of North Carolina at Chapel Hill, Chapel Hill, North Carolina 27599-3255

M. J. Peters

Department of Physics and Astronomy, Appalachian State University, Boone, North Carolina 28608

(Received 3 May 2004; accepted 22 July 2004)

Raman scattering measurements of single-walled carbon nanotubes prepared by laser ablation with Ni/Co catalyst show that samples that have not been purified have a graphitic mode frequency that is 8 cm^{-1} lower than that of samples from which most of the catalyst has been removed. The shift is attributed to charge transfer from the catalyst particles to the nanotubes. The charge transfer from the residual catalyst also affects the temperature dependence of the radial breathing mode. © 2004 American Institute of Physics. [DOI: 10.1063/1.1792805]

I. INTRODUCTION

In the dozen years since carbon nanotubes were discovered, Raman spectroscopy has emerged as an extremely useful tool for their characterization.¹ In single-walled nanotubes (SWNTs) the frequency of the radial breathing mode (RBM), a low-frequency A_{1g} symmetry vibration in which the atoms in the nanotube move purely in the radial direction, is strongly dependent on the diameter of the SWNT and therefore allows the diameter to be measured. At higher frequencies, the graphitic mode (GM) arises from vibrations of A_{1g} , E_{1g} , and E_{2g} symmetry (A_1 , E_1 , and E_2 in chiral tubes) in which the atoms move tangentially to the tube. This mode is closely related to the high-frequency E_{2g} mode in graphite, involving atomic motion within the graphite sheet, which is a sensitive probe of the charge transfer that occurs during the intercalation process.²

The various methods of fabrication of SWNTs,¹ including laser ablation, arc discharge, high-pressure disproportionation, and chemical vapor deposition, all involve the use of metal catalyst particles for the growth of the nanotubes. Purification by physical and chemical means removes some of the catalyst (along with amorphous carbon, fullerenes, and other byproducts of the synthesis), but achieving catalyst-free nanotube samples has proven to be very difficult. In the analysis of Raman scattering data from as-prepared samples, it is generally assumed that the spectrum is not affected by any charge transfer from a foreign species. It is therefore relevant to examine the effect of the residual catalyst on the Raman spectrum of SWNTs. We present here measurements of the Raman spectrum and its temperature dependence for SWNTs made with two different catalysts, with and without subsequent purification.

II. EXPERIMENT

The SWNTs were made by the method of laser ablation using a Nd:YAG (where YAG—yttrium aluminum garnet)

pulsed laser operating at 1000 mJ/pulse at a wavelength of 1064 nm. The furnace was held at a temperature of 1150 °C in an argon atmosphere of 200 SCCM (where SCCM denotes “cubic centimeter per minute at STP”). Three targets with different catalysts were used, two with different amounts of Ni/Co and one with Pd/Rh. The two Ni/Co targets were prepared with 0.75% and 0.3% each of Ni and Co. The target using Pd/Rh as a catalyst contained 0.6% Pd and 1.8% Rh. Details of the fabrication have been published elsewhere.³ Note that the catalyst concentration given is that of the ablation target, not the final nanotube sample (in either the unpurified or purified state).

The sample prepared with the 0.3% Ni/Co catalyst was subsequently purified. The purification process involved refluxing the sample in a hydrogen peroxide solution (20% for 9 h), sonicating in a carbon disulfide and methanol mixture (1:1) for 2 h, and finally filtering through a 2 μm membrane. The purification process has been extensively described elsewhere.⁴ The purified sample was then annealed at 1000 °C under vacuum for 1 h. Using x-ray diffraction XRD and TEM, the estimated purity of the resulting SWNT sample was found to be 90%.⁴ Based on previous experiments with samples similarly prepared, we expect that the tubes remain bundled, and that the residual catalyst particles are found predominantly at the ends of the tubes.

The Raman studies as a function of temperature were made using a Linkham THMS 600 heat stage. The temperature of the stage was monitored continuously. The average fluctuation in the temperature was ± 1.0 °C. Measurements were made in the temperature range from 300 to 750 K. Repeated heating cycles gave consistent results, indicating that no irreversible changes were taking place.

The Raman spectra were measured using a micro-Raman system attached to a Dilor XY triple spectrometer. The laser source used was a Coherent Innova 300 Ar⁺ laser operating at 514.5 nm. The microscope focused the incident beam to a spot size of $\approx 2\ \mu\text{m}$ and the backscattered light was collected 180° from the direction of incidence. The resolution of the spectrometer is 0.5 cm^{-1} . A charge-coupled device (CCD)

^{a)}Author to whom correspondence should be addressed; electronic mail: mcneil@physics.unc.edu

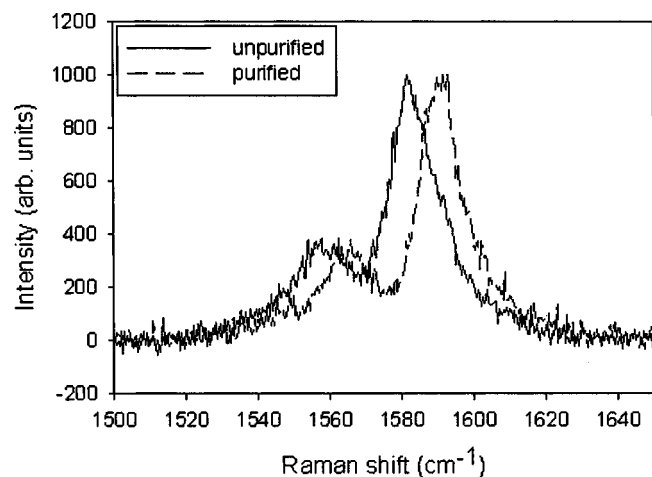


FIG. 1. Measured Raman spectrum at room temperature for unpurified and purified samples prepared with Ni/Co catalyst. Solid line: as-prepared. Dotted line: purified. Spectra have been normalized for comparison.

camera cooled with liquid nitrogen collected the data, which was then analyzed using a least-squares fit to a sum of Lorentzians.

III. RESULTS AND DISCUSSION

Raman spectra of the GM for the purified and unpurified Ni/Co samples at room temperature are shown in Fig. 1. The frequencies of the Raman modes as a function of temperature for the three samples are shown in Fig. 2, with the GM shown in Fig. 2(a) and the RBM in Fig. 2(b). The results of a linear fit of frequency vs temperature are given in Table I. The most striking observation is that the frequency of the GM at room temperature in the purified sample is substantially larger than for the unpurified samples, although the linewidths are very similar. This cannot result from the slightly different diameter distributions in the two samples, as the nanotube diameter has little effect on the frequency of the graphitic mode. The diameters of the resonant SWNTs in each sample were determined from the frequencies of the RBM,⁵ and despite the very different diameters of the nanotubes in the unpurified Ni/Co sample and the Pd/Rh sample, the frequencies of the GMs at room temperature are indistinguishable. The spectra of the purified sample also show no increase in the disorder-induced band near 1300 cm^{-1} compared to the unpurified samples, indicating that the purification process does not introduce a significant concentration of defects into the SWNTs.

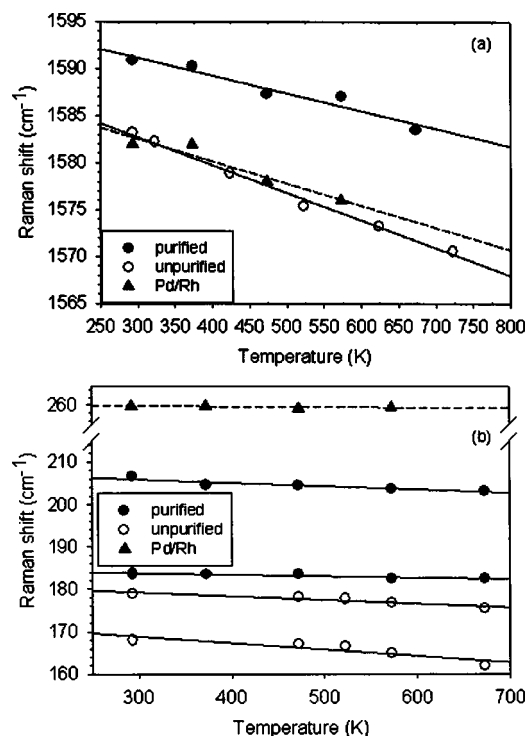


FIG. 2. (a) Graphitic mode frequency versus temperature for purified Ni/Co (filled circle), unpurified Ni/Co (open circle, solid line), and Pd/Rh (tri-angle, dashed line) samples, with linear fits. (b) Radial breathing mode frequency versus temperature for unpurified Ni/Co (open circle), purified Ni/Co (filled circle) and Pd/Rh (triangle) samples, with linear fits.

We attribute this shift in the GM frequency depending on the presence or absence of the metal catalyst particles to charge transfer from the residual metal catalyst to the SWNTs. It is reminiscent of the shifts observed in the corresponding vibrational mode in graphite intercalated with donor species such as alkali metals.² In graphite intercalation compounds, the presence of the transferred charge shifts the vibrational frequencies of the carbon layers upon which the excess charge resides (i.e., the bounding layers),⁶ splitting the single E_{2g} peak in the Raman spectrum into two peaks. One peak is produced by the carbon layers not adjacent to an intercalant layer (interior layers), and occurs at the frequency found in pure graphite. The other, produced by the bounding layers, is at a higher frequency. In the dilute (high-stage) limit, in which there are many additional carbon layers between each pair of bounding layers, the E_{2g} mode of the bounding layers has a frequency of 1613 cm^{-1} , compared to

TABLE I. Vibrational frequencies and their temperature dependences for various SWNT samples.

Sample	Nanotube diameter (nm)	RBM frequency at 300 K (cm^{-1})	Temperature coefficient of RBM (cm^{-1}/K)	GM frequency at 300 K (cm^{-1})	Temperature coefficient of GM (cm^{-1}/K)
0.75% Ni/Co (Unpurified)	1.37	169	-0.015 ± 0.001	1583	-0.030 ± 0.007
	1.30	179	-0.009 ± 0.001		
0.3% Ni/Co (Purified)	1.28	184	-0.004 ± 0.001	1591	-0.019 ± 0.007
	1.13	206	-0.008 ± 0.001		
Pd/Rh	0.89	260	-0.002 ± 0.002	1583	-0.024 ± 0.007

1582 cm^{-1} for the interior layers.⁷ In this limit, the transfer of 0.04 electrons per carbon atom in the bounding layer (assuming complete charge transfer from each alkali atom) produces an increase of 31 cm^{-1} in the Raman frequency. As the number of interior layers is reduced, so that the layers containing excess charge are brought closer together, the Raman frequency of the bounding layer in donor compounds decreases until it reaches $\approx 1603 \text{ cm}^{-1}$ in the stage 2 compound. In a stage 2 compound pairs of boundary layers are adjacent to one another with no intervening interior layers (so that all carbon atoms have on average 0.04 excess electrons). The downshift in frequency results from an in-plane lattice expansion in the bounding layers as the number of interior layers is reduced.⁸

For the vibrational mode in the nanotube that corresponds to the graphite E_{2g} mode, we observe a frequency difference of 8 cm^{-1} between the unpurified and the purified samples. This is comparable to the difference in bounding layer frequency between the dilute limit and stage 2 (10 cm^{-1}) or stage 3 (6.5 cm^{-1}). This suggests that the purified nanotube sample is comparable to the dilute (high-stage) intercalated graphite sample, and the unpurified sample to a graphite sample in which all or nearly all of the carbon atoms carry excess charge.

Deliberate alkali metal doping of carbon nanotubes (in contrast to the accidental doping due to residual catalyst considered here) results in a broadening and downshift of the graphitic mode, with a Breit-Wigner-Fano line shape at saturation.⁹ The downshift at saturation is typically $\sim 25 \text{ cm}^{-1}$ from the frequency observed in the as-prepared (not purified) sample in these experiments. It is clear that the accidental doping from residual catalyst involves considerably less total charge transfer (and therefore a smaller frequency shift) than the saturation state of deliberate donor doping. However, the effect is qualitatively the same. In deliberate doping experiments, the radial breathing mode has been observed not to shift in frequency as the doping proceeds,¹⁰ although the intensity of the peak is greatly reduced until it finally disappears. Because the frequency of the RBM is determined by the diameter,⁵ and different sample batches produced with different catalysts can produce nanotubes of different diameter, it is not possible here to meaningfully compare the frequencies of the RBMs of the unpurified and purified samples.

Our observation of charge transfer from residual catalyst particles is further reinforced by the linewidths we observe for the graphitic mode in our samples. Just as in the deliberately doped materials reported in the literature, here the sample with the greater degree of charge transfer (the unpurified sample) has the larger linewidth. At room temperature the GM linewidth for the unpurified sample, which has had charge donated to it by the residual metal catalyst particles, is almost 25% larger than that of the purified sample, which contains much less catalyst and therefore less transferred charge. This difference in linewidth between the (accidentally) doped and undoped samples persists at higher temperatures as the GM broadens in both samples, as can be seen in Fig. 3. The linewidths of the RBM at room temperature in the purified and unpurified samples are similar to each other

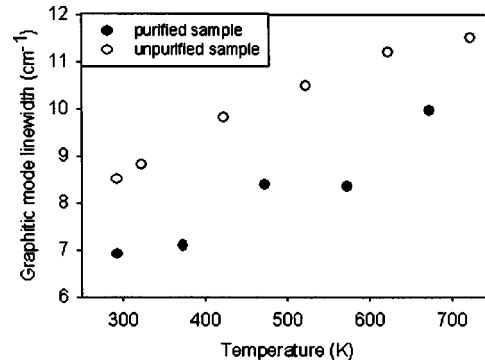


FIG. 3. Full width at half maximum of graphitic mode peak as a function of temperature for unpurified and purified samples prepared with Ni/Co catalyst. Open circles: unpurified Ni/Co sample. Solid circles: purified Ni/Co sample.

and to that of the GM of the purified sample, and there is little shift with temperature. This is consistent with doping studies that report no change in linewidth of the RBM as the doping proceeds.¹⁰

Both experimental and theoretical evidence for charge transfer between metallic dopants and SWNTs has been reported. Dopants that act as charge donors in graphite, such as K and Rb, have been observed to produce significant downward shifts of the graphitic mode frequency when intercalated into SWNTs,⁹ though changes in the Breit-Wigner-Fano line shape made the shifts difficult to quantify. In the same study, doping with Br_2 (which acts as an acceptor in graphite) produced an upshift of as much as 24 cm^{-1} . First-principles calculations of Li-intercalated SWNTs (Ref. 11) showed almost complete charge transfer from Li to the nanotube, and similar calculations with K produced charge transfers of as much as 0.8 electrons per K atom.¹²

To further support our contention that the softening of the graphitic mode in the unpurified samples is due to the residual metal catalyst particles, we have carried out first-principles pseudopotential calculations on interactions of SWNTs with all four catalyst metals (Ni, Co, Pd, and Rh). The density functional calculations were performed using plane-wave pseudopotential methods^{13,14} within the generalized gradient approximation.¹⁵ An ultrasoft pseudopotential¹⁶ was used to model the ion-electron interaction. A summary of the results of the calculation of Q , the charge transferred to the nanotubes (in fractions of the electron charge) and E_b , the binding energy between the metal ion and the nanotube (in eV), is shown in Table II. All of the metal atoms are found to be charge donors and show strong interactions with

TABLE II. Calculated charge transfers Q and interaction energies E_b between transition metal atoms and (9,0) nanotubes. Both quantities should be viewed qualitatively due to the small size of the unit cell (one metal atom per unit cell of nanotubes) used. Nevertheless, it is clear that all four metal catalyst atoms are charge donors to nanotubes. Calculations on tubes with different diameters and chiralities show similar results.

	Co	Ni	Pd	Rh
$Q(e)$	0.154	0.267	0.240	0.167
$E_b(\text{eV})$	-1.659	-2.020	-0.585	-2.925

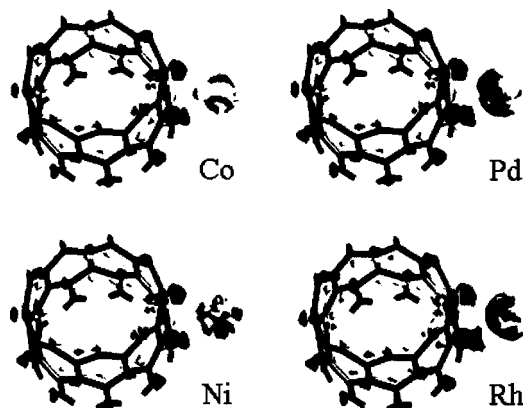


FIG. 4. Calculated net charge distribution in metal/nanotube complexes. The darker/lighter colors represent charge excess/deficit compared to the configuration in which the metal atoms are separated from the nanotube. This clearly shows that all four metals are charge donors, and that the excess charge is delocalized on the nanotubes.

SWNTs. Figure 4 shows the net charge distribution in the metal/nanotube complex for each of the four metals. The results clearly show that not only are all the metal atoms charge donors, but more importantly the donated charge is well delocalized on the nanotubes. Thus even though the catalyst metal atoms are not uniformly distributed in the nanotube samples, the effect of the charge transfer can be well delocalized such that a significant number of the carbon atoms in the nanotubes feel the effect of the charge transfer, resulting in the softening of the graphitic vibrational mode. These results indicate that the Ni/Co catalyst particles can be expected to transfer charge to the nanotubes, which would cause a downshift in the graphitic mode frequency with increasing amount of residual catalyst, as is observed in the present experiment. The unit cell used in the calculations, that of a (9,0) nanotube, contains 12 carbon atoms. The calculated charge transfers of 0.154–0.267 electrons therefore correspond to ≈ 0.01 –0.02 electrons per carbon atom. In graphite intercalated with alkali metals, the charge transferred from the intercalant layers is known to reside essentially entirely on the carbon layers adjacent to the intercalant layer (the bounding layers).⁶ A “stage 2” alkali metal intercalation compound, in which each pair of alkali metal layers is separated by two carbon layers, has a composition of $C_{24}M$ ($M=K, Rb, Cs$) and thus an alkali/carbon ratio of 0.04. If full charge transfer of one electron per alkali metal atom is assumed, then the number of transferred electrons per carbon atom would also be 0.04. The charge transfers of 0.01–0.02 electrons per carbon calculated here for these metal catalyst atoms are thus comparable to the charge transfer observed in graphite intercalation compounds.

These measurements and calculations together lead us to the conclusion that residual catalyst particles present in nanotube samples transfer enough charge to the nanotubes to affect the Raman spectrum. The GM of an as-prepared sample therefore is not characteristic of pure nanotubes, but rather is significantly downshifted due to the charge transfer.

A second significant observation from these data is that the breathing mode frequency shifts with temperature, as has been observed by others.^{17,18} Ravavikar *et al.* observed that

smaller-diameter tubes had larger temperature coefficients for the breathing mode, a trend opposite to that observed in our data. Their calculation found the temperature dependence of the breathing mode to be dominated by the softening of the intratubular C-C bond strength and the intertubular van der Waals interactions. The almost exact cancellation of the effect of the C-C bond length expansion and the bond-bending-related contraction kept the thermal expansion of the tube from contributing significantly to the change in the breathing mode frequency. In our data, the temperature dependence of the breathing modes of the tubes prepared with Pd/Rh catalyst is very small, despite the fact that these tubes have the smallest diameter of any measured in this study. Indeed, the temperature coefficient of the radial breathing mode is inversely correlated with the tube diameter in our data (though there is some scatter in the data).

One possible source for the differences in the temperature coefficients of the vibrational modes among these three studies is the different catalysts, as our comparison of the purified and unpurified Ni/Co samples suggests. The SWNTs measured by Ravavikar *et al.* were prepared by the HiPco process,¹⁹ in which Fe clusters formed by the decomposition of $Fe(CO)_5$ serve as catalysts for the growth of nanotubes from Co. Those measured by Li *et al.*¹⁸ were produced by arc discharge with a YNi_2 catalyst, whereas the SWNTs measured in this study were produced by laser ablation with either a Ni/Co or a Pd/Rh catalyst. The charge transfer from intercalation in graphite is known to induce changes in the bond lengths within the graphene sheet,²⁰ which shifts the vibrational frequencies. Different amounts of charge transfer per catalyst atom and different amounts of catalyst present, may produce different values for the shifts in the vibrational modes with temperature as a result of the different C-C bond lengths. Comparison of the temperature dependence measured here for the RBM of nanotubes of similar diameter (1.28 and 1.30 nm) but different amounts of Ni/Co catalyst suggests that the larger charge transfer that results from the larger amount of catalyst present in the unpurified sample gives a larger temperature dependence to the breathing mode. Comparison of the temperature dependences of the graphitic modes of the two samples suggests the same conclusion for the tangential vibrations.

IV. CONCLUSIONS

We have used Raman scattering to measure the frequency and temperature dependence of the radial breathing mode and the graphitic mode of single-walled carbon nanotubes prepared by laser ablation with two different catalysts. The frequency of the graphitic mode in the unpurified Ni/Co catalyst sample was 8 cm^{-1} lower than the corresponding mode in the sample from which most of the catalyst has been removed, which we attribute to charge transfer from the catalyst particles to the nanotubes. Our pseudopotential calculations predict a transfer of charge from Ni and Co atoms to the nanotube that is comparable to the charge transfer observed for graphite intercalated with alkali metal atoms. We conclude that Raman spectra of nanotubes from which the residual catalyst has not been removed are characteristic of

nanotubes interacting with dopant species, rather than of pristine nanotubes. The temperature dependence of the radial breathing mode was larger for nanotubes of larger diameter, contrary to what has been observed in previous studies. We attribute this to different amount of charge transfer in samples prepared with different catalyst materials, which results in changes in the C-C bond lengths and thus in the temperature dependence of the vibrational modes.

ACKNOWLEDGMENTS

The authors would like to thank C.-K. Yang for helpful discussions, L. Fleming for providing the nanotube materials, and J. Weinberg-Wolf and E. Harley for assistance with the Raman measurements. This work was supported by the Office of Naval Research under Grant No. N00014-98-1-0597.

- ¹See, for example, A. G. Souza Filho, A. Jorio, Ge. G. Samsonidze, G. Dresselhaus, R. Raito, and M. S. Dresselhaus, *Nanotechnology* **14**, 1130 (2003); M. S. Dresselhaus and P. C. Eklund, *Adv. Phys.* **49**, 705 (2000); R. Saito, G. Dresselhaus, and M. S. Dresselhaus, *Physical Properties of Carbon Nanotubes* (Imperial College, London, 1998), p. 183.
- ²M. S. Dresselhaus and G. Dresselhaus, in *Light Scattering in Solids III*, edited by M. Cardona and G. Güntherodt (Springer, New York, 1982), p. 3
- ³A. Thess *et al.*, *Science* **273**, 483 (1996).
- ⁴X.-P. Tang, A. Kleinhammes, H. Shimoda, L. Fleming, K. Y. Bennoune, S. Sinha, C. Bower, O. Zhou, and Y. Wu, *Science* **288**, 492 (2000).

- ⁵A. M. Rao, J. Chen, E. Richter, U. Schlecht, P. C. Eklund, R. C. Haddon, U. D. Venkateswaran, Y.-K. Kwon, and T. Tománek, *Phys. Rev. Lett.* **86**, 3895 (2001).
- ⁶S. A. Solin, in *Graphite Intercalation Compounds I*, edited by H. Zabel and S. A. Solin (Springer, Berlin, 1990), p. 157.
- ⁷S. A. Solin, *Mater. Sci. Eng.* **31**, 153 (1977).
- ⁸S. Y. Leung, G. Dresselhaus, and M. S. Dresselhaus, *Synth. Met.* **2**, 89 (1980).
- ⁹A. M. Rao, P. C. Eklund, S. Bandow, A. Thess, and R. E. Smalley, *Nature (London)* **388**, 257 (1997).
- ¹⁰N. Bendiab, L. Spina, A. Zahab, P. Poncharal, C. Marliere, J. L. Bantignies, E. Anglaret, and J. L. Sauvajol, *Phys. Rev. B* **63**, 153407 (2001).
- ¹¹J. Zhao, A. Buldum, J. Han, and J. P. Lu, *Phys. Rev. Lett.* **85**, 1706 (2002).
- ¹²C. Jo, C. Kim, and Y. H. Lee, *Phys. Rev. B* **65**, 035420 (2002).
- ¹³M. C. Payne, M. P. Teter, D. C. Allen, T. A. Arias, and J. D. Joannopoulos, *Rev. Mod. Phys.* **64**, 1045 (1992).
- ¹⁴CASTEP is a density functional theory package with the plane-wave pseudopotential method distributed by Accelrys Inc. V. Milman, B. Winkler, J. A. White, C. J. Pickard, M. C. Payne, E. V. Akhmatkaya, and R. H. Nobes, *Int. J. Quantum Chem.* **7**, 895 (2000).
- ¹⁵J. P. Perdew and Y. Wang, *Phys. Rev. B* **45**, 13244 (1992).
- ¹⁶D. Vanderbilt, *Phys. Rev. B* **41**, 7892 (1990).
- ¹⁷N. R. Raravikar, P. Keblinski, A. M. Rao, M. S. Dresselhaus, L. S. Schadler, and P. M. Ajayan, *Phys. Rev. B* **66**, 235424 (2002).
- ¹⁸H. D. Li *et al.*, *Appl. Phys. Lett.* **76**, 2053 (2000).
- ¹⁹M. J. Bronikowski, P. A. Willis, D. T. Colbert, K. A. Smith, and R. E. Smalley, *J. Vac. Sci. Technol. A* **19**, 1800 (2001).
- ²⁰D. E. Nixon and G. S. Perry, *J. Phys. C* **2**, 1732 (1969); A. Herold, in *Physics and Chemistry of Materials with Layered Structures*, Vol. 6, edited by F. Levy (Reidel, Dordrecht, 1979), p. 323.